RESEARCH PAPER

Green Approach to enhance cell viability of copper oxide nanoparticles in normal periodontal fibroblast cell line (In vitro study)

Marwa A. El-Saeed[1,2], Ghada Adayil[3], Hanan Eid Gamal Yousef[4,5]

[1]Lecturer of Oral Biology, Faculty of Dentistry, Cairo University, Egypt

[2]Lecturer of Oral Biology, Faculty of Dentistry, Misr University for Science and Technology (MUST) University, Egypt

[3]Lecturer of Periodontics, Faculty of Dentistry, Cairo University, Egypt

[4]Associate Professor of Oral and Maxillofacial Pathology, Faculty of Dentistry, Minia University, Egypt

[5]Associate Professor of Oral and Maxillofacial Pathology, Faculty of Oral and Dental Medicine, Nahda University, Egypt

Received: 25th May, 2026; **Revised:** 6th June, 2026; **Accepted:** 8th June, 2026; **Available Online:** 09th June, 2026

ABSTRACT

Background

Copper oxide nanoparticles (CuO-NPs) have extensive biomedical applications; however, their possible cytotoxicity may limit their application in periodontal tissues. Green synthesis could be a solution to improve their biocompatibility.

Aim

Evaluation of the effect of CuO-NPs produced in a green environment was the motivation for the current investigation prepared via Pomegranate peel extract (PPE) on the viability, inflammatory signaling, oxidative stress, and apoptotic markers in Human periodontal ligament fibroblast cells (PDL-1 cell line).

Materials and Methods

In contrast to chemically manufactured CuO-NPs, green CuO-NPs were prepared using phytochemicals obtained from pomegranates. To analyze the nanoparticles, scientists used X-ray diffraction (XRD), transmission electron microscopy (TEM), zeta potential, Fourier transform infrared spectroscopy (FTIR), and ultraviolet-visible spectroscopy (UV-Vis). The fibroblast cells found in the periodontal ligament were subjected to varying concentrations of CuO-NPs. Along with the measurement of IL-1β, NO, NF-κβ, Bcl-2, and Bax, we also measure nuclear factor kappa B (NF-κβ) to assess inflammatory, oxidative, and apoptotic responses. The MTT test is used to determine cytotoxicity.

Results

Green-synthesized CuO-NPs showed lower cytotoxicity and higher cell viability compared to chemically synthesized CuO-NPs. Fibroblasts maintained better morphology under microscopic examination. Green CuO-NPs also reduced nitric oxide, IL-1β, NF-κβ, Bax, and Bcl-2 levels, indicating lower oxidative stress, inflammation, and apoptotic activity.

Conclusion

These results indicate that copper oxide nanoparticles mediated by PPE may serve as a potential safer and more biologically friendly alternative in future periodontal biomedical applications.

Keywords: Green synthesis; Copper oxide nanoparticles; Periodontal ligament fibroblasts; Cell viability; Periodontal infection.

How to cite this article: El-Saeed MA, Adayil G, Yousef HEG. Green Approach to enhance cell viability of copper oxide nanoparticles in normal periodontal fibroblast cell line (In vitro study). Int J Drug Deliv Technol. 2026;16(57s): 1667-1680. DOI: 10.25258/ijddt.16.57s.166

Source of support: Nil.

Conflict of interest: None.

1. Introduction

Nanotechnology has captured the interest of researchers from various fields, especially biomedical sciences [1-3]. The distinctive physicochemical characteristics of nanoparticles (NPs), which are very tiny particles with a size range of 1–100 nanometers, have led to their use in a number of fields. Nanoparticles that have been engineered have found use in several domains, including engineering, industry, and the health sciences. [3, 4]. The tenacious emission of these NPs into the environment leads to their increased incorporation and subsequent contact with many beneficial non-human life forms, but, more significantly, human exposure, which arises through inhalational or gastrointestinal pathways. This info raises fears of possible cytotoxicity and unfavorable

effects upon human contact with nanoparticles. Nanoscale particles are considerably larger in their surface/volume ratio than the bulk phase, so they have different physicochemical properties that could show cytotoxicity as a function of conditions [4-7].

Among nanomaterials, nanoparticles based on metals, especially metal oxides are widely used. Copper (II) oxide nanoparticle (CuO-NP) serves as an important example of a nanomaterial is used in many different commercial and industrial goods because of its unique physicochemical properties; catalysts, solar cells, gas detectors, agrochemicals, paints, and antibacterial items are all part of their category. [8], electrochemical [9], photovoltaic [10], and photoconductive [11] characteristics. The public and regulatory agencies are very worried about the possible toxicological repercussions of the discharge of copper oxide nanoparticles (CuO-NPs) due to their quick introduction and broad presence in the environment. As a result, a lot of research has gone into trying to figure out if they are harmful to people and the environment. A sensitive route of exposure for CuO-NP includes inhalation and dermal exposures [12, 13]. Several studies have shown that part of the toxic effect of CuO-NPs results from the discharge of copper ions [14, 15]. A crucial determinant in the prediction of nanoparticle-mediated toxicity is the onset and kinetics of CuO nanoparticle dissolution since dissolved copper ions are implicated in toxicity [16, 17].

Middle to late decades of the last century, plenty of evidence has been provided over a variety of cell models supporting the cytotoxicity of CuO-NPs via oxidative stress, which occurs with subsequent DNA damage and death [18]. Moreover, animal model-based toxicological studies have shown that exposure to CuO-NP induces inflammation and liver damage [18, 19].

Nanoparticles of synthetic copper, which are used as active components in antifouling paints for ships and in agricultural biocides, may travel through the air and settle into soil. Beyond their direct discharge, airborne nanoparticles may also fall into natural water bodies and pollute the systems [14-16]. In addition, power plants, smelters, metal foundries, asphalt, inkjet printers, and rubber tires can also release metallic Cu nanoparticles to the environment. Under ambient conditions, they will oxidize to produce CuO nanoparticles. Dissolution can decrease particle size which increases the movement of particles. Such parameters are important for NP application in biomedicine because they may be directly related to cytotoxicity [10].

We found that CuO nanoparticles were the most poisonous and produced the most DNA damage, and we also showed that these effects were not caused by dissolved ions alone[11-13] Putting human bone marrow-isolated mesenchymal stem cells through their paces, nanoscale CuO was proved to be having 30 times stronger cytotoxicity relative to bulk CuO [15-18]. The results of these investigations strongly suggest that the toxicity of CuO particles varies significantly depending on their size. We investigate the effects of nanoparticles with diameters less than 100 nm on CuO toxicity and want to get a better knowledge of the role of particle size in relation to this substance based on these findings. [19].

Scaling and root planing are used to manage periodontitis; however, they remain ineffective in preventing the onset of dental caries due to weakened antibacterial activity at this bacterial concentration.[4] Cuo-NPs exhibit powerful antimicrobial activity fungus and other microbes, including both gram-positive and gram negative bacterica, but no studies have examined their antibacterial activity against any specific dental infection. Rationale for the use of Cuo-NP in antimicribial therapy would dictate a specific therapeutic time and concentration [20]. Moreover, Cuo-NPs are synthesized biogenically through eco-friendly materials such as microorganisms, plants and enzymes due to the cost-effectiveness, simplicity, and nontoxicity of these biochemical species [21–23].

Nanoparticles are synthesized using chemical, physical and most recently green approaches [18]. Numerous approaches have been reported for the green preparation of nanoparticles, such as biosynthesis, microwave heating, photocatalysis, magnetic-field-assisted technique and electrochemical techniques. Biosynthesis of nanoparticles is a strategy to make use of microbes or plants for manufacture of nanoparticles and have medicinal applications. An environmentally friendly alternative to traditional physical and chemical processes for producing nanoparticles has been developed. This has been described as a spot-on, simple-to-use, non-toxic, biocompatible, cost-efficient, safe, and eco-friendly technology [18]. Plant extracts notably contain phytochemicals, which act as reducing agents, and in some cases also stabilize or cap molecules that are needed for medical applications. Pomegranate peels are full of bioactive chemicals, especially flavonoids, phenolics, ellagitannins (ETs), proanthocyanins, several minerals, and complex polysaccharides etc. Reactive oxygen and nitrogen species are the primary causes of illness, and polyphenolic substances are utilized to prevent them. [24-27].

Although there have been a few research looking at how CuO-NPs affect the immune system, none have looked at how they affect the PDL-1 cell line. [11]. The purpose of this in vitro experiment is to determine whether or not the PPE-based green

manufacturing method improves the biocompatibility and cell survival of CuO-NPs when tested in the PDL-1 cell line.

2. Materials and methods

The study consists of 3 main groups:

Group 1: Untreated control including Human Periodontal ligament Fibroblast Cells (PDL-1).

Group 2: (PDL-1) cells treated with chemically synthesized CuO (CuO-NPs).

Group 3: (PDL-1) cells treated with Green Synthesized PPE-CuO-NPs.

2.1 Materials

Copper acetate dihydrate with absolute ethanol (Loba-Chemie, India). The German company Merck supplied the sodium hydroxide. The human periodontal ligament fibroblast cells (PDL-1 Cell Line; ATCC® CRL-1882) were obtained from the American Type Culture Collection (ATCC; Manassas, VA, USA). Every cell line was cultured and tested for cytotoxicity at Al-Azhar University's Regional Center for Mycology and Biotechnology's Tissue Culture Unit. Sigma (St. Louis, MO, USA) provided the Trypan blue dye, MTT, and DMSO. The following items were purchased from Lonza (Belgium): fetal bovine serum, DMEM, HEPES buffer solution, gentamycin, L-glutamine, and 0.25 percent Trypsin-EDTA.

2.2 Preparation Methods:

Pomegranate peel extract (PPE) is derived from pomegranate fruit grown in Egypt and is commercially available for human consumption. We measured 85 grams of the fruit and mixed it with 100 milliliters of distilled water to make pomegranate extract. The grinding process was followed by boiling the mixture at 80 °C for six hours and filtering it through paper.

2.2.1. Green Synthesized PPE-CuO-NPs

The nanoparticles were produced using copper acetate and pomegranate leaf extract. A process of oxidation was initiated by dissolving 60 grams of leaves in one liter of deionized water at 353 K with stirring for approximately one hour. Then, a 1:2 (v/v) ratio of the suspended leaves with a 0.2 M Copper acetate dihydrate solution was added to start the sample production. This could have happened because Cu(OH)2 was formed when copper acetate plus the hydroxyl anion (OH) in water responded. The CuO nanoparticles were obtained by drying the pellets at 323 K for twenty-four hours. Following this, they were rinsed three times with distilled water, crushed, and passed through a 500 µm screen filter. [28].

2.2.2. Chemically synthesized CuO-NPs

Nanoparticles of copper oxide were synthesized using the sol-gel technique. There are a number of advantages to this approach for stabilizing nanoparticles that have been manufactured. Following standard procedures, CuO nanoparticles were synthesized using the chemical precipitation method [19]. The process of creating CuO-NPs began with the dissolution in ethanol of 9.0 grams of copper (II) acetate dihydrate and 5.4 grams of sodium hydroxide pellets, which were then mixed. Each component, sodium hydroxide and copper (II) acetate dihydrate, was dissolved in its own little volume of ethanol. While stirring continuously at room temperature (25 degrees Celsius), a sodium hydroxide solution was added to a copper(II) acetate dihydrate solution in small increments. The copper hydroxide that was precipitated had a dark brown color. Using a centrifuge (Hermle ZHK 32, Germany), the precipitate was filtered. Following this, the drying equipment was used to dry the precipitate at a temperature of around 50 degrees Celsius. To get crystalline CuO nanoparticles, the dehydrated material was further heated to 600˚C by annealing. The next step was to anneal the material before grinding it into nanoparticle powder. The following is a schematic representation of the chemical procedure that was used to characterize CuO nanoparticles using the powdered sample:

$Cu(CH_3COO)_2 + 2NaOH \rightarrow Cu(OH)_2 + 2CH_3COONa$.

2.3 Characterization techniques:

The XRD pattern of the sample using the XPERT-PRO Powder Diffractometer system, 2Theta (20^O - 80^O), minimum step size = 0.001, Wavelength (Kα) =1.54614^O

The morphological examinations were carried out with a 200 kV accelerating voltage using a high-resolution transmission electron microscope (TEM) from Thermo Scientific, the Talos F200i. To prepare the TEM sample, 3 µl of the colloidal solution was dropped onto a copper grid that was coated with Formvar (Ted Pella) and allowed to evaporate at room temperature. The Zetasizer Nano ZS (Malvern Instruments, UK) was used to measure the zeta potential and particle size. Before and between measurements, the samples were sonicated after being stabilized overnight at room temperature. Bruker Analytical, Germany's Vertex 70-RAM II spectrometer was used to acquire ATR/FTIR spectra from the produced compounds. FTIR/ATR spectra were obtained at ambient temperature on a scale of 400-4000 cm⁻¹. The Cary series UV-Vis-NIR, from Australia, was used to assess the optical characteristics.

2.4 Biological assays:

2.4.1 Cell viability assay (MTT assay)

The cell cultures were maintained in a medium that included DMEM with the following

additives: ten percent heat-inactivated fetal bovine serum, one percent L-glutamine, HEPES buffer, and 50 µg/ml of gentamicin. The cells were cultivated every other week at 37 degrees Celsius in a humidified chamber with five percent carbon dioxide. The cells were seeded into a 96-well plate with 100 µL of growth medium, with a density of 1×10^4 cells per well.

After 24 hours after seeding, a 96-well flat-bottom microtitre plate (Falcon, NJ, USA) was used to create a fresh medium containing six concentrations of the test material. This was then pipetted into the wells containing confluent cell monolayers.Every concentration of the test substance was assigned three wells on the microtiter plates, which were kept at 37 degrees Celsius in a humidified incubator with five percent carbon dioxide for twenty-four hours. The test chemical was not present in the cultures of the control cells.After incubation for twenty-four hours, the number of viable cells was determined using the MTT test.

After 100 µL of fresh RPMI 1640 culture medium, which did not include phenol red, was added to the 96-well plate, the media was removed, and 10 µL of a 12 mM MTT stock solution, with five milligrams of MTT per well (including the untreated control wells with PBS), was added. The 96-well plates were then placed in an incubator set at 37°C with 5% CO2 for a duration of four hours. After removing 85 µl of media from the wells, 50 µl of DMSO was added to every well. After ten minutes of incubation at 37°C, the liquid was vortexed using a pipette.

The optical density at 590 nm (OD value) was measured using a microplate reader (SunRise, TECAN, Inc, USA). Wells with 100% viability were defined as those containing only viable cells. To calculate the viability percentage, the formula [(ODt/ODc)]×100% was used, where ODt is the mean OD of wells treated with the experimental sample. Odc stands for the average optical density of cells that have not been treated.

After the tested cell line is treated with the specified chemical, the survival curve is shown as a function of drug concentration. The dose-response curve was analyzed using nonlinear regression to get the cytotoxic concentration (CC50), which is the concentration required to destroy fifty percent of intact cells according to concentration. The Graphpad Prism program was used for data analysis (San Diego, CA, USA). [29].

2.4.2 Microscopic Observation of the periodontal ligament fibroblast cell line treated with the compounds:

The method described before was used to conduct an experiment. The inverted plates were rinsed three times with 300 µl of phosphate-buffered saline (pH 7.2) after treatments at the prescribed concentration. Cells were then adhered to the plates using ten percent formalin for fifteen min at temperature in the room. The cells that had been fixed were then stained for Twenty minutes with 100 µl of 0.25 percent crystal violet. To rinse plates, remove excess discoloration, and let them dry, deionized water is utilized.

An inverted microscope (CKX41; Olympus, Japan) with a digital microscopy camera was used to analyze cellular morphology and assess morphological changes in comparison to control cells. At 200x and 400x magnifications, alterations in morphology indicative of cytotoxic effects were seen under the microscope..

2.4.3 Cell culture

Gentamicin (fifty µg/ml), ten percent heated-inactivated fetal bovine serum, one percent L-glutamine, HEPES buffer, and DMEM were all used to grow the cells. Cells were cultivated at 37ºC in a humidified environment with five percent carbon dioxide and subcultured on a weekly basis. The Experiment was conducted in order to assess whether the tested sample could protect Human Periodontal ligament fibroblasts cells (PDL-1 cell line; ATCC® CRL-1882) against damage induced by Lipopolysaccharide (LPS). The sample was incubated with PDL-1 cells for 2 h, followed by stimulation with LPS (10 µg/ml [30,31] for 24 h, at which time IL-1beta and NO levels were determined to evaluate the inflammatory responses, as described above.

2.4.4 Cell treatment

All green-synthesized CuO nanoparticles were administered to periodontal fibroblast cells at doses between -2 and 25 µg/mL for a 24-hour incubation period. Untreated cells: used as negative controls. The systemic treatments were applied under sterile conditions.

On 24-well tissue cultivation plates, human periodontal ligament fibroblast cells (PDL-1 cell line) were grown at a density of 5×10^5 cells/mL. When a complete monolayer of cells has grown in every well of the plate, the tested substance was introduced into 24-well tissue single-use wells, informed by cytotoxicity data, alongside cell controls (under cell culture conditions). Triplicate cuvettes were established for each treatment. The cells were collected twenty-four hours after therapy by aspirating the culture medium, trypsinizing them for twenty min at a concentration of 0.25 percent, centrifuging them for five min, and then washing them twice in Twenty-minute bursts of Phosphate Buffered Saline (PBS). They examined several inflammatory indicators assessed in HSF-1 cell pellets (treated vs untreated). The assessment of inflammatory markers (cytokines)

was conducted as previously outlined, using ELISA colorimetric kits in accordance with the manufacturer's instructions.

2.4.5 Human Interleukin 1beta (IL-1β) ELISA Kit

One of the methods used by the ELISA Kit is the Sandwich-ELISA. This kit's Microelisa strip plate already has an IL-1 BETA-specific antibody applied to it. A specific antibody is mixed with standards or samples and then added to the appropriate wells of a Microelisa strip plate. Afterwards, a particular antibody to IL-1 BETA that has been covalently coupled with Horseradish Peroxidase (HRP) is added to each well of the Microelisa strip plate and left to incubate. Components that are not bound are removed. After that, the TMB substrate solution is added to every single well. The wells that were blue before adding the stop solution became yellow; these wells contain IL-1 BETA, which is an HRP-conjugated antibody. The spectrophotometric measurement of optical density is performed at a wavelength of 450 nm. The levels of interleukin-1 beta (IL-1β) have a direct correlation with the optical density (OD) value. [32].

2.4.6 Measurement of Nitric Oxide

With the use of an available for purchase colorimetric Nitric Oxide Assay Kit (Cat—no E-BC-K035, Elabscience, Houston, TX, USA), we were able measure indirect NO generation by observing nitrite (NO_2^-), a stable metabolic consequence of NO. After forty-eight hours of treatment, the cell culture supernatants were collected and spun at 1,000 × g for ten min at four degrees Celsius to remove any cell debris. They were then either processed right away or stored at −80 °C for future analysis. The concentration of nitrite was determined by following the manufacturer's instructions for the Griess reaction. This procedure involves reacting nitrite with sulfanilamide and N-(1-naphthyl) ethylenediamine to form a stable purple azo product. The 96-well plate was prepared by adding the Griess reagents and sample in equal proportions. The mixture was then allowed to incubate at the ambient temperature, covered with a light cloth, for fifteen minutes. The absorbance at 540 nm was measured using a microplate reader. A standard curve was prepared by serially diluting the sodium nitrite standard that included with the kit. Subtracting the NO concentrations from the standard curve, the samples were then expressed as µmol/L. [33].

2.4.7 Measurement of NF-κβ, Bcl-2, and Bax

A quantitative in vitro study of the serum inflammatory marker NF-□ was carried out using the Human NF-β ELISA kit (Catalog No: MBS450580). For each of the kit's reagents and standards, we painstakingly followed the manufacturer's instructions. The color variations were determined by using spectrophotometric measurements at 450 nm. The B-Cell Leukemia/Lymphoma 2 (Bcl2) and proapoptotic marker (Bax) were measured using assays developed and manufactured by Cloud-Clone Corp, USA, with the reference numbers SEB343Hu Human HO1 and SEA778Hu, respectively.

2.5 Statistical analysis:

In order to assess the results, which were presented as mean ± SD, we utilized GraphPad Prism (version 8.0; GraphPad Software, Inc., San Diego, California, USA) and one-way evaluation of variance (ANOVA) with Tukey analysis for multiple comparison. The findings were considered statistically significant when the value of p was 0.05 or lower.

3 Results

3.1 Physicochemical Characterization:

On display in Figure 1 are the X-ray diffractograms of CuO-NPs, PPE, and PPE-CuO-NPs. To summarize, a wide peak at roughly 20:25 ° suggested an amorphous structural character of the various kinds of amorphous carbon materials [34].

The diffraction pattern of the chemically as well as green synthesized CuO-NPs exhibited peaks at 2θ = 32.5, 35.40, 38.70, 38.9,46.2,48.7,53.5,58.26 and 61.5 were assigned to reflection lines of monoclinic CuO nanoparticles. The monoclinic crystallite structure is further verified by diagrams of the different crystal planes, such as (020), (021), (110), (002), (111), (042), (130) and so forth. The absence of foreign peaks indicated the preparation of high-quality CuO-NPs.

In contrast to the chemical CuO, which has a gap in the optical band of 1.3-3.3 eV and a wide absorption peak between 300 and 400 nm, the pomegranate peel extract shows a higher absorption in the UV region (200–350 nm). Moreover, the PPE-CuO exhibited the absorption bands of pristine CuO and PPE, which confirmed that a homogeneous conjugation and compounding between them took place.

The chemical conjugation of CuO with PPE was investigated by FTIR experiments, which analyzed the FTIR spectrum of PPE **(Fig. 1c).** In CuO-NPs that were chemically produced, characteristic absorption bands corresponding to the Cu-O stretching vibration were detected in the 400-650 cm^{-1} range., as compared with reference spectra, confirming their purity and that the purification process removed foreign ions or elements, which were absent from their peaks [35]. Moreover, the FTIR spectrum of PPE showed Wide bands of strong intensity at 3316 cm−1 for pomegranate peel, attributed to the stretching of alcohols, phenols, and carboxylic acids, which involve O–H vibrations in pectin, lignin, and cellulose, influential constituents of PPE. Carbohydrates primarily consist of hydroxyl groups per 6-carbon

atom & methyl groups, that cause the methoxy group's C-H stretching to be accompanied by peaks at 3300 cm^{-1} and 1363 cm^{-1}. The stretching of the carbonyl (C=O) bond is supported by the bands at 1719 cm^{-1}, which provide credence to the presence of aldehydes, ketones, and carboxylic acids [36]. Further, the presence of biomolecules responsible for its complex structure is indicated by the various absorption bands seen in the FTIR spectrum of PPE-CuO-NPs. It is believed that this is caused by the vibrational frequencies of the Cu-O bonds, which manifest at 423 and 517 cm^{-1}. At 1038 cm^{-1}, the H-OH stretching frequency peaked, and at 1727 cm^{-1}, the carboxyl group was discernible. An expansive absorption band centred at 3327 cm1 was associated with the -OH group in the FTIR study; this group is mostly present on the surfaces of CuO nanostructures.

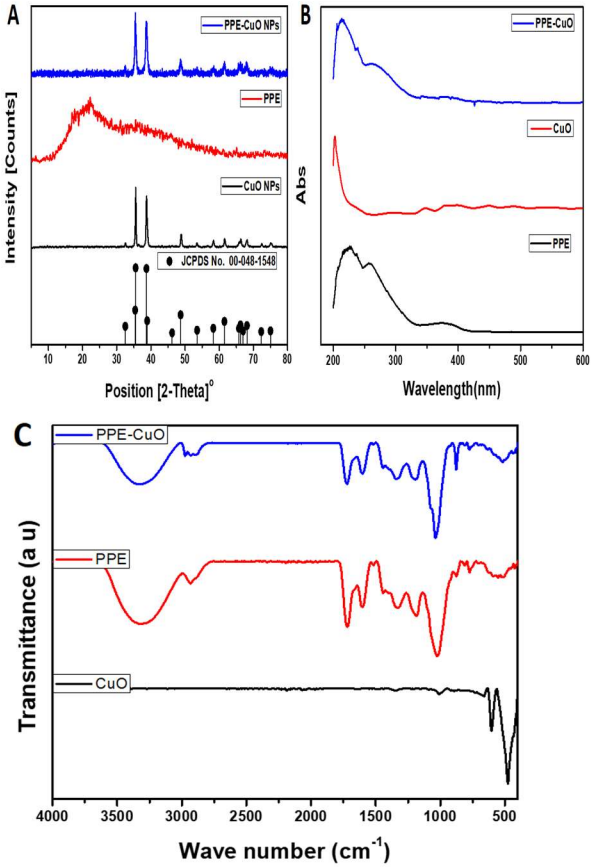

Fig. 1. The XRD patterns, Optical absorption, and FTIR of chemically synthesized CuO-NPs, Green synthesized CuO-NPs, and PPE—a, b, and c, respectively.

Transmission electron microscopy (TEM) images **Fig. 2** of the synthesized CuO nanoparticles showed nanoscale particles with an average diameter of 35 ± 5 nm, predominantly spherical morphology, and a small degree of agglomeration due to their comparatively higher surface energy. Furthermore, the zeta potential of PPE-CuO-NPs displayed a negative charge (- 21.6 ± 0.99 mV) due to conjugation with flavonoids and phenolic compounds of PPE **Fig. 3**.

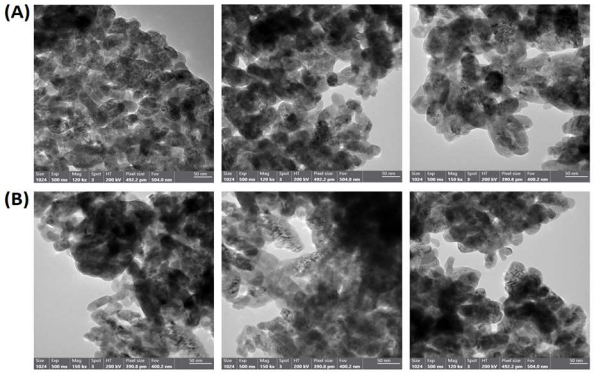

Fig. 2. The TEM images of A) Chemically synthesized CuO-NPs and B) Green synthesized CuO-NPs, respectively.

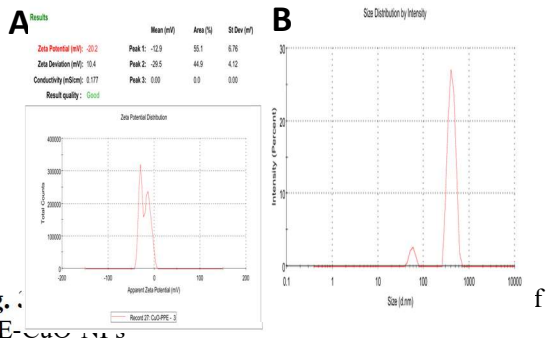

Fig. 3 f PPE-

3.2 MTT assay:

The cell viability experiment indicated that the proportion of viable cells decreased with increasing concentrations of CuO-NPs. Furthermore, the PPE-CuO-NPs exhibit a greater proportion of viable cells in comparison to the chemically synthesized CuO-NPs. As seen in Fig. 4. The examined material demonstrated cytotoxicity at the assessed doses when analyzed in the PDL-1 cell line with the MTT assay for 24 hours under the specified experimental conditions. The Cytotoxic Concentration (CC50) refers to the concentration necessary to induce toxic effects in fifty percent of PD-L1 cells. The average CC50 of chemical CuO-NPs and PPE-CuO-NPs are 18.78±1.12 and 82.77 µg/mL, respectively. Demonstrating a favorable safety profile of CuO-NPs after the conjugation with PPE.As shown in **Table 1**.

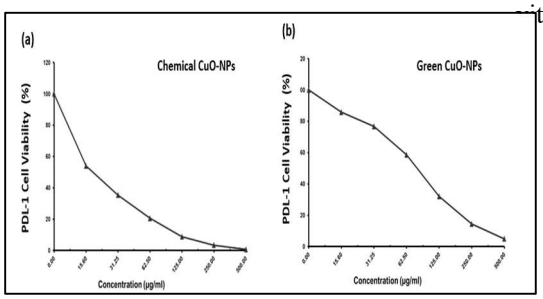

Fig. 4. Cell viability (%) of the effect of (**a**) chemically synthesized and (**b**) green-synthesized CuO-NPs on the PDL-1 cells. P<0.001

Table 1: The evaluated material demonstrated harmful effects contingent upon the tested doses when assessed for its cytotoxicity on the normal human periodontal ligament fibroblast (PDL-1) cell line using the MTT assay under experimental circumstances for twenty-four hours. The Cytotoxic quantity (CC_{50}) is the quantity necessary to induce toxic effects in 50% of PD-L1 cells.

Sample code	CC_{50} (µg/ml) (3 Replicates)			Mean CC_{50} (µg/ml)	S.D. (±)
	1st	2nd	3rd		
Chemical CuO-NPs	18.29	17.98	20.07	18.78	1.12
Green CuO-NPs	82.01	86.90	79.40	82.77	3.81

Additionally, the microscopic examination of cells treated with CuO nanoparticles and PPE-CuO nanoparticles in comparison to untreated cells as illustrated in **Fig. 5 and Fig. 6**.

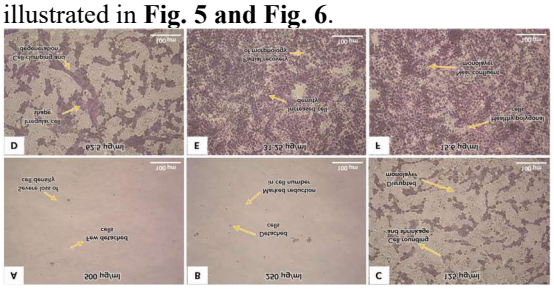

Fig. 5. PDL-1 cells treated with chemically synthesized CuO-NPs at 500, 250, 125, 62.5, 31.25, 15.6 µg/ml concentration, A, b, c, d, e, and f, respectively magnification 200x. G) PDL-1 cells, non-treated (control), magnification 400x.

Overall, the results demonstrate a clear concentration-dependent cytotoxic effect of chemically synthesized CuO-NPs on PDL-1 cells. Higher nanoparticle concentrations induced severe cellular damage, loss of viability, and altered morphology, whereas lower concentrations preserved cellular integrity and proliferation capacity. These findings support the notion that CuO-NP toxicity increases proportionally with nanoparticle concentration.

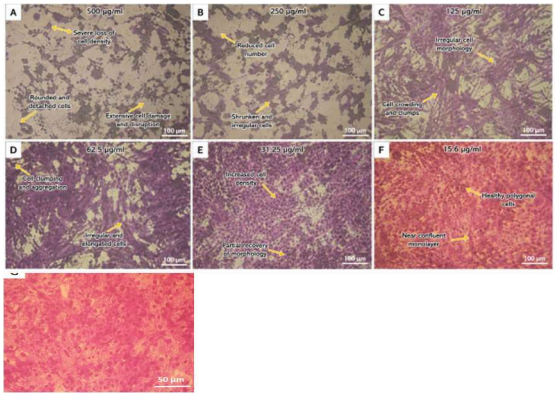

Fig. 6. PDL-1 cells treated with Green synthesized CuO –NPs at 500, 250, 125, 62.5, 31.25, 15.6 µg/ml concentration, A, b, c, d, e, and f, respectively. Magnification 200x.

PDL-1 cells treated with green synthesized CuO-NPs exhibited concentration-dependent morphological alterations. At higher concentrations (500 and 250 µg/ml; panels A and B), marked cytotoxicity was observed, including severe reduction in cell density, rounded and detached cells, and disruption of the cellular monolayer. Moderate concentrations (125 and 62.5 µg/ml; panels C and D) showed irregular cell morphology, cellular aggregation, and partial degeneration with elongated and distorted cells. In contrast, lower concentrations (31.25 and 15.6 µg/ml; panels E and F) demonstrated improved cellular integrity, increased cell density, and near-normal polygonal morphology, indicating reduced cytotoxic effects and partial recovery of PDL-1 cells.

3.3 Effect of CuO-NPs and PPE-CuO-NPs on NO level, IL-1β produced by LPS-stimulated macrophages

LPS stimulation clearly increased NO and IL-1β production, indicating a robust inflammatory response of macrophages. Both nitric oxide and IL-1β levels were significantly reduced with CuO-NPs treatment compared to the control group. PPE-CuO-NPs exhibit a larger reduction in these inflammatory mediators than chemically synthesized CuO-NPs. The results show significantly lower levels of nitric oxide and IL-1β production in the PPE-CuO-NPs group, suggesting improved anti-inflammatory and antioxidant effects as in **Fig. 7.** ANOVA showed that nitric oxide level ($F = 303.261$, $p < 0.0001$) was high significant differences between all groups, green CuO-NPs (PPE-CuO-NPs) had the lowest mean value at 2.2 ± 0.1, whereas the control group recorded the greatest

mean value at 3.8 ± 0.2. G1 compared to G2 (P = 0.001), G1 compared to G3 (P < 0.001), and G2 compared to G3 (P = 0.013), all of which were shown to have statistically significant differences according to the post-hoc Tukey test. The control group had the highest mean value (26 ± 1) and the group treated with green CuO-NPs (PPE-CuO-NPs) had the lowest mean value (14 ± 0.5), indicating that there were significant variations in the IL-1β level across all groups (F = 793.577, p < 0.0001). There were significant differences across all groups, as shown by the post-hoc Tukey test: G1 against G2 (P < 0.001), G1 compared G3 (P < 0.001), and G2 versus G3 (P = 0.002).

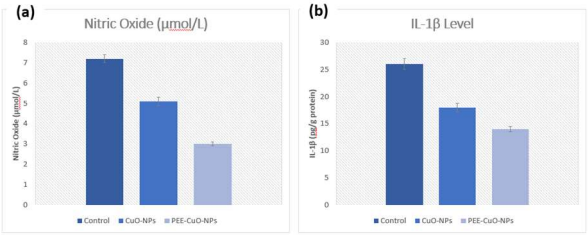

Fig. 7. Effect of CuO-NPs and PPE-CuO-NPs on Nitric oxide level (a) and interleukin-1β (IL-1β) (b) produced by LPS-stimulated macrophages

3.4 Impact of CuO-NPs and PPE-CuO-NPs on the Expression Levels of NF-κB, Bcl-2, and BAX in Human Periodontal Ligament Fibroblast Cells.

The effects of CuO-NPs and PPE-CuO-NPs on the expression levels of apoptotic, anti-apoptotic and inflammatory markers in PDL-1 cells are showed in **Fig. 8**.

One-way ANOVA indicated substantial disparities among the groups for the expression of the anti-apoptotic marker Bcl-2 (F = 14.787, p = 0.0048), with the control group exhibiting the greatest mean value (5.0 ± 0.4) and the green CuO-NPs (PPE-CuO-NPs) group displaying the lowest mean value (2.5 ± 0.5). The post-hoc Tukey test indicated a statistically significant difference between G1 and G2 (P = 0.003) and between G1 and G3 (P < 0.001). ANOVA indicated that BAX expression (F = 127.300, p < 0.0001) exhibited very significant differences across all groups, with the greatest mean value observed in the control group (420 ± 25), and the lowest mean value noted in the green CuO-NPs (PPE-CuO-NPs) group (190 ± 12). There were statistically significant variations across all groups, according to the post-hoc Tukey test: G1 against G2 (P > 0.001), G1 compared G3 (P < 0.001), and G2 versus G3 (P = 0.002).

ANOVA analysis of NF-κB expression revealed very significant differences across all groups (F = 64.364, p < 0.000088), with the control group exhibiting the greatest mean value (7.2 ± 0.6) and the green CuO-NPs (PPE-CuO-NPs) group displaying the lowest mean value (3 ± 0.3). The post-hoc Tukey test indicated statistically significant differences across all groups: G1 versus G2 (P = 0.003), G1 vs G3 (P < 0.001), and G2 vs G3 (P = 0.003). **Fig. 8** and **Table 2.** The decreased NF-κβ level indicates that inflammatory signaling is suppressed, and the drop in BAX and Bcl-2 expression indicates alterations in apoptosis-related pathways, thereby enhancing cellular homeostasis.

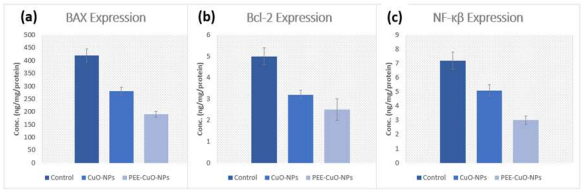

Fig. 8. Effect of CuO-NPs and PPE-CuO-NPs on BAX (a), Bcl-2 (b), and NF-κβ (c) expression levels in Human Periodontal ligament fibroblasts cells.

Utilizing GraphPad Prism version 8.0 (GraphPad Software Inc., San Diego, CA, USA), a one-way assessment of variance (ANOVA) was performed, followed by Tukey's post hoc multiple comparative test. Mean ± standard deviation (n = 3) is used to display the data. At p < 0.05, statistical significance was determined. As in shown in the following **Table 2.**

Table 2: ANOVA and Post-Hoc Tukey of the experimental groups

Parameter	Groups	Mean (± SD)	F-value	p-value	Post-hoc Tukey Test (p-value)
Nitric Oxide (µmol/L)	Control (G1) CuO-NPs (G2) PPE-CuO-NPs (G3)	3.8 ± 0.2 2.8 ± 0.2 2.2 ± 0.1	305.261	<0.0001**	G1 vs G2 equal 0.001* G1 vs G3 less than 0.001* G2 vs G3 equal

					0.013*
IL-1β (pg/g protein)	Control (G1) CuO-NPs (G2) PPE-CuO-NPs (G3)	26 ± 1 18 ± 0.8 14 ± 0.5	793.577	<0.0001**	G1 vs G2 less than 0.001* G1 vs G3 less than 0.001* G2 vs G3 equal 0.002*
BAX Expression	Control (G1) CuO-NPs (G2) PPE-CuO-NPs (G3)	420 ± 25 280 ± 15 190 ± 12	127.300	<0.0001**	G1 vs G2 less than 0.001* G1 vs G3 less than 0.001* G2 vs G3 equal 0.002*
Bcl-2 Expression	Control (G1) CuO-NPs (G2) PPE-CuO-NPs (G3)	5.0 ± 0.4 3.2 ± 0.2 2.5 ± 0.5	14.787	0.0048*	G1 vs G2 equal 0.003* G1 vs G3 less than 0.001* G2 vs G3 equal 0.147
NF-κβ Expression	Control (G1) CuO-NPs (G2) PPE-CuO-NPs (G3)	7.2 ± 0.6 5.1 ± 0.4 3.0 ± 0.3	64.364	0.000088**	G1 vs G2 equal 0.003* G1 vs G3 less than 0.001* G2 vs G3 equal 0.003*

4 Discussion:

The clinical use of chemically synthesized CuO-NPs nanoparticles as a therapeutic agent remains challenging due to their high cytotoxicity, oxidative stress, and the inflammatory responses they evoke in normal cells. Utilizing GraphPad Prism version 8.0 (GraphPad Software Inc., San Diego, CA, USA), a one-way assessment of variance (ANOVA) was performed, followed by Tukey's post hoc multiple comparative test.. To address these limitations, green synthesis strategies have been proposed as eco-friendly and biocompatible alternatives. In this approach, pomegranate-derived phytochemicals serve as stabilizing agents to produce nanoparticles with improved surface properties, lower toxicity, and greater biocompatibility. Consequently, green-synthesized CuO-NPs nanoparticles can be considered a safe biomedical candidate for periodontal therapy [39-41].

The physicochemical characterizations, including XRD, FTIR, optical absorption, and Zeta potential, confirm a successful synthesis and conjugation of CuO-NPs with PPE, and There was a considerable difference in the cell viability of CuO-NPs and PP-CuO-NPs. The dose at which PDL-1 cell

development in culture medium is fifty percent inhibited compared to spontaneously occurring cells was measured as the half cytotoxic concentration [CC50].

The above findings were also validated by synthesizing chemically produced CuO nanoparticles and PPE-CuO nanoparticles. XRD patterns exhibited distinct diffraction peaks indicative of the monoclinic phase of CuO, therefore validating the synthesis of stable, crystalline CuO nanoparticles. An existence of functional groups of phytochemicals from pomegranate peel on the surface of the nanoparticles was verified by FTIR study, confirming their functions as minimizing, stabilizing, and capping substances. The spherical form and average size of the nanoscale CuO nanoparticles, as shown by TEM investigation, were 35 ± 5 nm. This result signifies that bioactive surface-modified CuO-NPs nanoparticles were effectively manufactured by a green method, exhibiting improved stability and biological compatibility.

The study *in vitro* investigates the impact of a periodontal ligament fibroblast cell line on the act as the last number of conventional approaches towards utilizing green-synthesized CuO-NPs added to it, on surviving cells, and its biocompatibility.

CuO-NPs and PPE-CuO-NPs had CC_{50} of 18.78±1.12 and 82.77 µg/mL for PDL-1, respectively. Two well-established processes from the literature may be responsible for CuO's cytotoxicity. According to the first mechanism [42-44], The capacity of copper oxide to produce reactive oxygen species (ROS) is what causes its toxicity; these ROS then interact with DNA and lipids, two macromolecules found in cells, and lead to cell death. On the other hand, the second method proved that CuO nanoparticles and the cell's lysosome penetrated directly [45, 46]. Because of a high level of bioactive substances, such as antioxidants, phenolic compounds (such as tannins and flavonoids), and phytic acids, PPE-CuO-NPs have a notable safety impact. Chemical and metal-assisted (green) nanosynthesis techniques were used to create various CuO nanoparticles; one device exposed the nanoparticles directly to human tissues. In the present study, researchers found that newly green-synthesized CuO-NPs exhibited significantly greater biocompatibility than chemically synthesized CuO-NPs.

Chemically generated CuO nanoparticles and PPE-CuO nanoparticles were tested for their cytotoxic effects on the PDL-1 cell line in an MTT assay, which showed a response that was dependent on concentration. Noticeably less cytotoxicity was caused by PPE-CuO-NPs compared to CuO that was chemically generated.

Green CuO-NPs had a CC_{50} value of 82.77 ± 3.81 µg/ml, while the CC_{50} value of chemical CuO-NPs was a considerably lower 18.78 ± 1.12 µg/ml. This suggests that green-synthesized nanoparticles were less toxic and improved fibroblast cell viability compared to chemically synthesized CuO-NPs. The lower toxicity of PPE-CuO-NPs can be attributed to the bio-coating provided by pomegranate peel extracts, including phenolic compounds, flavonoids, tannins, and antioxidant constituents. These bioactive molecules can not only form a protective layer around the nanoparticles, thereby reducing their toxic interactions with cellular components, but also improve biocompatibility with normal periodontal ligament fibroblast cells. Our results were in accordance with the cytotoxicity of CuO-NPs, assessed by Khalifa & Hussien [40], which reduced the viability of cancer cells in a dose-dependent manner. The major cause of this cytotoxicity is the excessive creation of ROS inside cells, which causes oxidative stress and damage to the mitochondria [30]. Also, CuO nanoparticles slowed the proliferation of cancer cells and caused ROS-mediated death. Due to nanoparticle-induced flaws and smaller particles, the present research found better cytotoxicity which, as shown in this work, promote increased ROS production and, consequently, higher cellular internalization.

The heightened cytotoxicity of chemically synthesized CuO-NPs may be ascribed to established toxicity mechanisms linked to copper oxide nanoparticles, marked by excessive generation of reactive oxygen species and the liberation of toxic Cu^{2+} ions following nanoparticle dissociation upon interaction with the lysosome. These pathways may inflict harm on cellular proteins, lipids, and DNA, resulting in mitochondrial malfunction, inflammation, and cellular apoptosis. The harmful impact of pomegranate peel on microorganisms was diminished by the fermented PPE-CuO-NPs, likely due to the antioxidant and stabilizing capabilities of herbal biomolecules from pomegranate peel present on the surface of the metal nanoparticles. In this study, the biological behavior of CuO nanoparticles was influenced not only by size but also primarily by environmental conditions, owing to their surface chemistry and production process.

Moreover, the anti-inflammatory findings also reaffirmed the ideal biological performance of PPE-CuO. LPS stimulation increased nitric oxide production and IL-1β levels, indicating a pronounced inflammatory response. Both CuO-NPs and PPE-CuO-NPs treatments decreased these inflammatory mediators, but PPE-CuO-NPs treatment resulted in a greater reduction than the chemically synthesized counterpart. This indicates that pomegranate peel-

mediated CuO nanoparticles exhibited stronger anti-inflammatory and antioxidant effects. This effect, as is well known, may be attributed to the potential of pomegranate peel phytochemicals to counteract oxidative stress and to interrupt inflammatory signaling pathways that regulate NF-κβ-related responses.

Moreover, the expression of NF-κβ, Bcl-2, and BAX suggested that PPE-CuO-NPs may act as a protector in Human Periodontal ligament fibroblasts cells. Reductions in pro-inflammatory and pro-apoptotic markers, along with increased cell viability, demonstrated that PPE-CuO-NPs reduced cellular stress, apoptosis, and inflammation more effectively than chemically synthesized CuO-NPs. These findings show that pomegranate peel extract (Natural polyphenols) can serve as a protective template for the green synthesis of CuO nanoparticles, thereby enhancing their biological safety profile and making them potential candidates for biomedical applications and tooth remineralization (periodontal diseases).

The work by Khalifa and Hussien [40] indicated that chemically manufactured or doped CuO-NPs resulted in increased apoptosis, mostly via heightened caspase-3 activation, overexpression of Bax, and downregulation of Bcl-2, which was mediated by excessive ROS generation. This aligns with the findings of Ueno et al. [48], who elucidated the involvement of caspase-3 signaling pathways in oxidative stress-induced mitochondrial impairment. The pro-apoptotic protein Bax was overexpressed, but the critical anti-apoptotic protein Bcl-2 was drastically downregulated. An elevated Bax/Bcl-2 ratio results in mitochondrial membrane permeabilization, the liberation of cytochrome c, and thus, programmed cell death. Pilco-Ferreto and Calaf [33] indicated that a comparable apoptotic pattern was noted, wherein the Bax/Bcl-2 equilibrium is crucial in oxidative stress-induced apoptosis of cancer cells.

This suggests inhibition of the mitochondrial apoptosis pathway. By comparison, chemically synthesized CuO nanoparticles have been demonstrated to stimulate apoptosis via Bax activation and a co-upregulation of Bcl-2, as well as caspase-dependent signaling cascades culminating in programmed cell death [49].

In addition, pro-inflammatory cytokines such as IL-6 were decreased in response to green CuO-NPs, resulting in a lower inflammatory response. Such results suggest that possible green synthesis may be less upregulated in the inflammatory signaling pathways. On the other hand, Khalifa & Hussien [40] demonstrated that ROS-dependent mechanisms mediated the major changes in inflammatory mediators, such as IL-1β, after treatment with CuO nanoparticles, which were often associated with increased cellular stress and inflammation. Notably, the observed reduction in IL-1β levels indicates inhibition of pro-inflammatory signaling pathways critical for tumor development. This anti-inflammatory action may result from the disruption of ROS-mediated cytokine synthesis. Furthermore, nanoparticle treatment led to a significant decrease in nitric oxide generation after stimulation with IFN-γ or PMA combined with ionomycin, indicating the suppression of inducible nitric oxide synthase (iNOS) activity. Prajapati et al. [35] published same findings, indicating that reactive nitrogen species (RNS) produced by nanoparticles of various metal oxides, including TiO2, ZnO, and CuO, might diminish nitric oxide levels and inflammatory responses via the modulation of oxidative stress pathways.

In addition, green CuO-NPs reduced IL-1β levels significantly during the inflammatory response assessment, suggesting that pro-inflammatory signaling pathways were inhibited. This is especially relevant for periodontal applications, given the key role of chronic inflammation in disease progression. In contrast, chemically synthesized nanoparticles induced higher levels of inflammatory cytokines, leading to tissue stress and cell dysfunction.

Furthermore, cells treated with green CuO-NPs also had significantly lower oxidative stress markers, indicating reduced NO levels. This indicates that green-synthesized nanoparticles cause less oxidative stress than chemically synthesized ones. On the other hand, chemically synthesized CuO nanoparticles are associated with high levels of ROS production, which causes oxidative damage, mitochondrial dysfunction, and subsequent apoptosis [50, 51]. This suggests a decrease in oxidative stress induction and in the activation of inducible nitric oxide synthase (iNOS). On the other hand, chemically synthesized CuO nanoparticles are known to promote ROS and NO, both of which are upstream mediators of DNA damage [51], mitochondrial dysfunction and apoptosis [52].

5 Conclusion

In conclusion, our study showed that a green-synthesized CuO-NPs prepared from PPE are more biocompatible and less cytotoxic than chemically synthesized CuO-NPs. They enhanced the viability of the PDL-1 cell line, lowered levels of inflammatory mediators such as NO, IL-1β, and NF-κβ in the PDL-1 cell, and regulated apoptosis-related markers, including Bcl-2 and BAX. Pomegranate peel extract-mediated copper oxide nanoparticles could be a safer and more effective way for periodontal biomedicine in the future as well.

6 Recommendation:

In vivo and clinical studies would be needed to validate the safety and bioactivity of green-

synthesized copper oxide nanoparticles in periodontal applications.

Ethical approval:
All techniques in this trial received approval from the Research Ethics Committee (REC) of the Faculty of Oral and Dental Medicine at Nahda University. (Approval number: 007-4-26-2).

Consent for publication

Since the article doesn't contain any personal information, consent to publish was not required. The submission of this work for publication and its contents have the full support of all authors.

Data Availability
Included in this published publication are all data produced or analyzed in this inquiry. Upon reasonable request, you may also get them from the corresponding author.

Declaration of competing interest:
There are no known conflicts of interest between the authors' personal connections or financial interests that may have influenced the results of this research, the authors state.

Funding statement
The manuscript received no funds.

Credit authorship contribution statement
Marwa A. El-Saeed: Writing – review & editing, Methodology, Validation, Formal analysis, Data curation, Conceptualization. **Ghada Adayil**: Writing – original draft, Methodology, Formal analysis, Data curation. **Hanan Eid Gamal Yousef:** Writing – review & editing, Methodology, Investigation, Formal analysis, Data curation, Validation, Supervision.

References

1. Mahmoud, N.M.R., Mohamed, H.I., Ahmed, S.B. *et al.* (2020). Efficient biosynthesis of CuO nanoparticles with potential cytotoxic activity. *Chem. Pap.* 74, 2825–2835. https://doi.org/10.1007/s11696-020-01120-6.
2. Marwa A. El-Saeed, Ghada Adayil, Mohamed A. Hazzaa, Mostafa Salah Hussein El Mallwany (2024). Exploring the Oral Microbiome: Implications for Peri-Implant success" A systematic Review and Meta-analysis. Journal of Carcinogenesis, 23(1), 942-956. https://doi.org/10.64149/J.Carcinog.23.1.942-956.
3. Elsaeed, Marwa & Korany, Nahed & Ezzat, Bassant. (2021). COMPARATIVE STUDY OF TOXIC EFFECT OF DIFFERENT SIZES OF SILVER NANOPARTICLES ON SUBMANDIBULAR SALIVARY GLAND, IN VIVO. Naz S, Gul A, Zia M. Toxicity of copper oxide nanoparticles: a review study. IET Nanobiotechnol. 2020;14(1):1-13.
4. El-Rab SMFG, Basha S, Ashour AA, Enan ET, Alyamani AA, Felemban NH. (2021). Green Synthesis of Copper Nano-Drug and Its Dental Application upon Periodontal Disease-Causing Microorganisms. J Microbiol Biotechnol. 28;31(12):1656-1666. doi: 10.4014/jmb.2106.06008. PMID: 34489380; PMCID: PMC9706032.
5. Emam MH, Nageh H, Ali F, Taha M, ElShehaby HA, Amin R, Kamoun EA, Loutfy SA, Kasry A. (2022). Inhibition of SARS-CoV-2 spike protein entry using biologically modified polyacrylonitrile nanofibers: in vitro study towards specific antiviral masks. RSC Adv. 31;12(25):16184-16193. doi: 10.1039/d2ra01321e. PMCID: PMC9155179.
6. Habib, S., Sadek, H., Hasanin, M., & Bayoumi, R. (2021). Antimicrobial Activity, Physical Properties and Sealing Ability of Epoxy Resin-Based Sealer Impregnated with Green Tea Extract-Chitosan Microcapsules: An In-Vitro Study. *Egyptian Dental Journal*, *67*(3), 2309-2319. doi: 10.21608/edj.2021.64866.1526
7. Benguigui, M., Weitz, I.S., Timaner, M. et al. (2019). Copper oxide nanoparticles inhibit pancreatic tumor growth primarily by targeting tumor initiating cells. Sci Rep 9, 12613. https://doi.org/10.1038/s41598-019-48959-8
8. Esmaeili Govarchin Ghaleh H, Zarei L, Mansori Motlagh B, Jabbari N. (2019). Using CuO nanoparticles and hyperthermia in radiotherapy of MCF-7 cell line: synergistic effect in cancer therapy. Artif Cells Nanomed Biotechnol. 47(1):1396-1403. doi: 10.1080/21691401.2019.1600529. PMID: 30964344.
9. Reddy ARN, Lonkala S. (2019). In vitro evaluation of copper oxide nanoparticle-induced cytotoxicity and oxidative stress using human embryonic kidney cells. Toxicol Ind Health. 35(2):159-164. doi: 10.1177/0748233718819371. PMID: 30803393.
10. Knight ET, Liu J, Seymour GJ, Faggion CM Jr, Cullinan MP. (2016). Risk factors that may modify the innate and adaptive immune responses in periodontal diseases. Periodontol 2000. 71(1):22-51. doi: 10.1111/prd.12110. PMID: 27045429.
11. Galdiero S, Falanga A, Vitiello M, Cantisani M, Marra V, Galdiero M. (2011). Silver nanoparticles as potential antiviral agents. Molecules. Oct 24;16(10):8894-918. doi: 10.3390/molecules16108894. PMID: 22024958; PMCID: PMC6264685.
12. Elsaesser A, Howard CV. (2012). Toxicology of nanoparticles. Adv Drug Deliv Rev. Feb;64(2):129-37. doi: 10.1016/j.addr.2011.09.001. Epub 2011 Sep 8. PMID: 21925220.
13. Singh G, Beddow J, Mee C, Maryniak L, Joyce EM, Mason TJ. (2017). Cytotoxicity Study of Textile

Fabrics Impregnated With CuO Nanoparticles in Mammalian Cells. Int J Toxicol. 36(6):478-484. doi: 10.1177/1091581817736712. PMID: 29153030.
14. Katsumiti A, Thorley AJ, Arostegui I, Reip P, Valsami-Jones E, Tetley TD, Cajaraville MP. (2018). Cytotoxicity and cellular mechanisms of toxicity of CuO-NPs in mussel cells in vitro and comparative sensitivity with human cells. Toxicol In Vitro. 48:146-158. doi: 10.1016/j.tiv.2018.01.013. PMID: 29408664.
15. Ren G, Hu D, Cheng EW, Vargas-Reus MA, Reip P, Allaker RP. (2009). Characterisation of copper oxide nanoparticles for antimicrobial applications. Int J Antimicrob Agents. 2009 Jun;33(6):587-90. doi: 10.1016/j.ijantimicag.2008.12.004. PMID: 19195845.
16. Applerot G, Lellouche J, Lipovsky A, Nitzan Y, Lubart R, Gedanken A, Banin E. (2012). Understanding the antibacterial mechanism of CuO nanoparticles: revealing the route of induced oxidative stress. Small. 5;8(21):3326-37. doi: 10.1002/smll.201200772. PMID: 22888058.
17. Naika HR, Lingaraju K, Manjunath K, et al. (2015). Green synthesis of CuO nanoparticles using Gloriosa superba L. extract and their antibacterial activity. J Taibah Univ Sci. 9(1):7-12. ISSN 1658-3655,https://doi.org/10.1016/j.jtusci.2014.04.006.
18. Pendashteh A, Mousavi MF, Rahmanifar MS. (2013). Fabrication of anchored copper oxide nanoparticles on graphene oxide nanosheets via an electrostatic coprecipitation and its application as supercapacitor. Electrochim Acta. 2013;88:347-357. 10.1016/j.electacta.2012.10.088.
19. Djurišić AB, Leung YH, Ng AM, et al. (2015). Toxicity of metal oxide nanoparticles: mechanisms, characterization, and avoiding experimental artefacts. Small.11(1):26-44.
20. Wang Z, Li N, Zhao J, White JC, Qu P, Xing B. (2012). CuO nanoparticle interaction with human epithelial cells: cellular uptake, location, export, and genotoxicity. Chem Res Toxicol. 25(7):1512-1521.
21. Kawasaki M. (2011). Laser-induced fragmentative decomposition of fine CuO powder in acetone as highly productive pathway to Cu and Cu2O nanoparticles. J Phys Chem C. 115(12):5165-5173. Doi: 10.1021/jp1095147.
22. Abdollahzadeh MR, Meshkatalsadat MH, Pouramiri B. (2023). Synthesis and characterization of copper nanoparticles utilizing pomegranate peel extract and its antibacterial activity. Int J New Chem.10(1):98-107.
23. Alaghehband R, Tavanaei L. (2025). Evaluation of antimicrobial effects of copper-zinc oxide nanocomposites biosynthesized by pomegranate peel on some pathogenic bacteria. Int J New Findings Health Educ Sci.;3(2):73-96.
24. Siddiqui MA, Alhadlaq HA, Ahmad J, Al-Khedhairy AA, Musarrat J, Ahamed M. (2013). Copper oxide nanoparticles induced mitochondria mediated apoptosis in human hepatocarcinoma cells. PLoS One. 5;8(8):e69534. doi: 10.1371/journal.pone.0069534.
25. Podstawczyk D, Pawłowska A, Bastrzyk A, Czeryba M, Oszmiánski J. (2019). Reactivity of (+)-catechin with copper (II) ions: the green synthesis of size-controlled sub-10 nm copper nanoparticles. ACS Sustain Chem Eng. 7:17535–17543. doi:10.1021/acssuschemeng.9b05078
26. Moschini E, Colombo G, Chirico G, Capitani G, Dalle-Donne I, Mantecca P. (2023). Biological mechanism of cell oxidative stress and death during short-term exposure to nano CuO. Sci Rep. 13(1):2326.
27. Vidovix, T.B., et al. (2019). Green synthesis of copper oxide nanoparticles using Punica granatum leaf extract applied to the removal of methylene blue. Materials Letters. 257: p. 126685.
28. Mosmann T. (1983). Rapid colorimetric assay for cellular growth and survival: application to proliferation and cytotoxicity assays. J Immunol Methods. 65:55-63.
29. Wollborn J, Wunder C, Stix J, Neuhaus W, Bruno RR, Baar W, Flemming S, Roewer N, Schlegel N and Schick MA. (2015). Phosphodiesterase-4 inhibition with rolipram attenuates hepatocellular injury in hyperinflammation in vivo and in vitro without influencing inflammation and HO-1 expression. J Pharmacol Pharmacother 6: 13-23.
30. Xiong W, Ma H, Zhang Z, Jin M, Wang J, Xu Y and Wang Z. (2019). The protective effect of icariin and phosphorylated icariin against LPS-induced intestinal epithelial cells injury. Biomed Pharmacother 118: 109246.
31. Selman, L. et al. (2012). An enzyme-linked immunosorbent assay (ELISA) for quantification of human collectin 11 (CL-11, CL-K1). J. Immunol. Methods 375, 182-188.
32. Bryan, N. S. & Grisham, M. B. (2007). Methods to detect nitric oxide and its metabolites in biological samples. Free Radic. Biol. Med. 43, 645-657
33. Pilco-Ferreto N, Calaf GM. (2016). Influence of doxorubicin on apoptosis and oxidative stress in breast cancer cell lines. International Journal of Oncology. 49(2):753–762. doi:10.3892/ijo.2016.3558.
34. Luna I., Hilary L., Chowdhury, A. , Gafur, M. , Khan, N. and Khan, R. (2015) Preparation and Characterization of Copper Oxide Nanoparticles Synthesized via Chemical Precipitation Method. Open Access Library Journal, 2, 1-8. doi: 10.4236/oalib.1101409
35. Nuhanović, M., et al. (2021). Pomegranate peel waste biomass modified with H3PO4 as a promising

sorbent for uranium (VI) removal. Journal of Radioanalytical and Nuclear Chemistry. 328(2): p. 617-626).
36. Abdelmigid, H.M., et al. (2022). Green synthesis of zinc oxide nanoparticles using pomegranate fruit peel and solid coffee grounds vs. chemical method of synthesis, with their biocompatibility and antibacterial properties investigation. Molecules, 27(4): p. 1236
37. Siddiqui, V.U., et al. (2021). Green synthesis of copper oxide (CuO) nanoparticles by Punica granatum peel extract. Materials Today: Proceedings. 36: p. 751-755
38. Tolkou, A.K., et al. (2024). Sustainable use of low-cost adsorbents prepared from waste fruit peels for the removal of selected reactive and basic dyes found in wastewaters. Environmental Science and Pollution Research. 31(10): p. 14662-1468.
39. Al-Fa'ouri, A. M., Abu-Kharma, M. H., Awwad, A. M., & Abugazleh, M. K. (2023). Investigation of optical and structural properties of copper oxide nanoparticles synthesized via green method using Bougainvillea leaves extract. Nano-Structures & Nano-Objects, 36, 101051.
40. Khalifa MM, Hussien NA. (2026). Anticancer and anti-inflammatory potentials of doped CuO and ZnO nanoparticles: a multi-pathway mechanistic study. Open Chemistry. 24(1):20250225.
41. Dolati M, Tafvizi F, Salehipour M, Komeili Movahed T, Jafari P. (2023). Biogenic copper oxide nanoparticles from Bacillus coagulans induced reactive oxygen species generation and apoptotic and anti-metastatic activities in breast cancer cells. Scientific Reports. 13:3256. doi:10.1038/s41598-023-30436-y.
42. Gaetke, L. M., & Chow, C. K. (2003). Copper toxicity, oxidative stress, and antioxidant nutrients. Toxicology, 189(1-2), 147-163.
43. Azizi M., Ghourchian H., Yazdian F., Dashtestani F. & AlizadehZeinabad H. (2017). Cytotoxic effect of albumin coated copper nanoparticle on human breast cancer cells of MDA-MB 231. PloS one, 12(11), e0188639.
44. Benguigui, M., Weitz, I.S., Timaner, M. et al. (2019). Copper oxide nanoparticles inhibit pancreatic tumor growth primarily by targeting tumor initiating cells. Sci Rep 9, 12613 https://doi.org/10.1038/s41598-019-48959-8
45. Studer AM, Limbach LK, Van Duc L, Krumeich F, Athanassiou EK, Gerber LC, Moch H, Stark WJ. (2010). Nanoparticle cytotoxicity depends on intracellular solubility: comparison of stabilized copper metal and degradable copper oxide nanoparticles. Toxicol Lett. 1;197(3):169-74. doi: 10.1016/j.toxlet.2010.05.012.
46. Midander K., Cronholm P., Karlsson H. L., Elihn K., Möller L., Leygraf C. & Wallinder, I. O. (2009). Surface characteristics, copper release, and toxicity of nano-and micrometer-sized copper and copper (II) oxide particles: a cross-disciplinary study. Small, 5(3), 389-399.
47. Ryter SW, Kim HP, Hoetzel A, Park JW, Nakahira K, Wang X, et al. (2007). Mechanisms of cell death in oxidative stress. Antioxid Redox Signal. 9:49–89.
48. Ueno M, Kakinuma Y, Yuhki K, Murakoshi N, Iemitsu M, Miyauchi T, et al. (2007). Doxorubicin induces apoptosis by activation of caspase-3 in cultured cardiomyocytes in vitro and rat cardiac ventricles in vivo. Journal of Pharmacological Sciences. 101(2):151–158. doi:10.1254/jphs.fp0050980
49. Ahamed, Maqusood & Alhadlaq, Hisham & Khan, M. & Akhtar, Mohd. (2012). Selective killing of cancer cells by iron oxide nanoparticles mediated through reactive oxygen species via P53 pathway. Journal of Nanoparticle Research. 15. 10.1007/s11051-012-1225-6.
50. Prajapati BG, Sharma D, Elossaily GM, Sharma N, Bilandi A, Kapoor DU. (2024). Unlocking potential of zinc oxide nanoparticles in enhancing topical drug delivery. Nano-Structures & Nano-Objects.39:101302. doi:10.1016/j.nanoso.2024.101302
51. Mroz RM, Schins RP, Li H, Jimenez LA, Drost EM, Holownia A, MacNee W, Donaldson K. (2008). Nanoparticle-driven DNA damage mimics irradiation-related carcinogenesis pathways. Eur Respir J. Feb;31(2):241-51. doi: 10.1183/09031936.00006707.
52. Shafagh M, Rahmani F, Delirezh N. (2015). CuO nanoparticles induce cytotoxicity and apoptosis in human K562 cancer cell line via mitochondrial pathway, through reactive oxygen species and P53. Iran J Basic Med Sci. 18(10):993-1000. PMID: 26730334; PMCID: PMC4686584.